Cationic Rhodium Complexes with Hemilabile Phosphine Ligands as Polymerization Catalyst for High Molecular Weight Stereoregular Polyphenylacetylene

M. Victoria Jiménez,* Jesús J. Pérez-Torrente,* M. Isabel Bartolomé, Eugenio Vispe, Fernando J. Lahoz, and Luis A. Oro

Departamento de Química Inorgánica, Instituto Universitario de Catálisis Homogénea, Instituto de Ciencia de Materiales de Aragón, Universidad de Zaragoza-C.S.I.C., 50009-Zaragoza, Spain.

AUTHOR EMAIL ADDRESS vjimenez@unizar.es, perez@unizar.es

Abstract

A series of cationic complexes $[Rh(diene)\{Ph_2P(CH_2)_nZ\}][BF_4]$ (diene = 1,5-cyclooctadiene (cod), tetrafluorobenzobarralene (tfb) or 2,5-norbonadiene (nbd)) containing functionalized phosphine ligands of the type $Ph_2P(CH_2)_nZ$ (n = 2, or 3; Z = OMe, NMe_2, SMe) have been prepared and characterized. These complexes have shown a great catalytic activity for phenylacetylene (PA) polymerization. Catalyst screening and optimization have determined the superior performance of complexes containing a P,N-functionalyzed phosphine ligand, $[Rh(diene)\{Ph_2P(CH_2)_3NMe_2\}]$ $[BF_4]$ (diene = cod **5**, tfb **6**, nbd **7**), and tetrahydrofuran as solvent. The influence of the diene ligand and the effect of temperature, PA to rhodium molar ratio, addition of water or a co-catalyst, DMAP (4-(dimethylamino)pyridine), have been studied. Diene ligands strongly influence the catalytic activity and complexes **6** and **7** are far more active than **5**. Both complexes gave polyphenylacetylene (PPA) with very high number-average molecular weights (M_n) of 970 000 (**6**) and 1 420 000 (**7**). The addition of DMAP resulted in a dramatic drop in the PPA molecular weight, 106 000 (**6**) and 233 000 (**7**,). The PPA obtained with the system **6**/DMAP showed a narrow molecular weight distribution (M_w/M_n = 1.20) and incremental monomer addition experiments have demonstrated the quasi-living nature of the polymerization reaction under these conditions. The PPA obtained with these catalytic systems has been characterized by ^{1}H and ^{13}C$\{^1$H$\}$ NMR spectroscopy and shows a *cis-transoidal* configuration with a high level of steroregularity (*cis* content superior to 99%). TGA, DSC, and IR analysis have revealed a thermal *cis*↔*trans* isomerization process at 150 ºC. The mechanism of PA polymerization has been investigated by spectroscopic means, under stoichiometric and catalytic conditions, and shows an active role of the hemilabile phosphine ligand both in the initiation and, probably, in the termination steps through proton transfer processes involving the hemilabile fragment of the ligand.

Introduction

Organic polymers displaying electrical conducting properties constitute an interesting class of materials for technological applications.[1] Transition metal-mediated polymerization of acetylene derivatives generates polyenes with π-conjugated backbones. The best known member within this family, polyacetylene, has been widely investigated because of its satisfactory conducting properties, though these materials are unstable in air and show low solubility in common solvents. In contrast, polymers based on substituted acetylenes are stable in air but display low conducting values as a consequence of the deviation from a planar structure induced by the substituents that decrease the π electron delocalization. The chemical and physical properties of polyphenylacetylene (PPA) are intermediate between those of polyacetylene and other substituted polyacetylenes. PPA is soluble in common organic solvents, is stable in air and displays semi-conductor properties. The conductivity strongly depends on the *cis/trans* content of the polymer; the conductivity of the polymer with a *trans* configuration is about ten orders of magnitude higher than the polymer with a *cis* configuration.[2] In addition to electrical conductivity, other physical properties such as photoconductivity, optical nonlinearity, liquid crystallinity, gas-selective permeability, or magnetic susceptibility could also be of special importance in such materials.[3]

Several well-established transition-metal based catalyst for the polymerization of substituted acetylenes have been developed, as for example, Ziegler-type catalysts,[4] two-component metathesis polymerization catalysts[5] or well-defined transition metal Schrock-type carbene complexes.[6] Although there are several initiators that induce stereospecific living polymerization of polyacetylenes,[7] in general, the reactions are not stereoselective and give mixture of *cis* and *trans* polymers.[8] The reactivity of rhodium(I) complexes towards aromatic substituted acetylenes includes dimerization, cyclization and oligomerization, depending both on the structure of the acetylene and the reaction conditions.[9] Noteworthy, rhodium catalysts are also efficient for the polymerization of monosubstituted acetylenes with formation of highly stereoregular polymers, in some cases in a living manner.[10]

The pioneering work reported by Furlani[11] showed that cationic rhodium(I) complexes [Rh(cod)(N-N)]$^+$ (N-N = bipy, phen), in the presence of a strong base, such as NaOH, were efficient catalysts for the polymerization of phenylacetylene (PA). In contrast, the complexes [Rh(Tp^{R2})(cod)] (Tp^{R2}; Tp = tris-pyrazolylborate, R = Me, Ph, *i*-Pr),[12] [Rh(diene){(η^6-C$_6$H$_5$)BPh$_3$}] (diene = cod,[13a] nbd[13b]), among others,[14,15] were found to exhibit high catalytic activity without any co-catalyst. On the other hand, Noyori and coworkers have reported the living polymerization of PA using the complex [Rh(C≡CPh)(nbd)(PPh$_3$)$_2$] or the system [Rh(μ-OMe)(nbd)]$_2$/PPh$_3$ in the presence of DMAP.[16] Living polymerization was also achieved by the multicomponent catalytic system [Rh(μ-Cl)(nbd)]$_2$/Ph$_2$C=CPhLi/PPh$_3$,[17] and the vinyl complexes [Rh{C(Ph)=CPh$_2$}(diene)(PR$_3$)].[18,19]

We have recently become interested in the design of hemilabile ligands for transition metal catalytic applications.[20] The most important property of hemilabile ligands is the reversible protection of one or more coordination sites. In this context, functionalized phosphines have been intensively studied as hemilabile ligands for soft metal centers because of their ability for providing easily accessible coordination vacancies through a potentially dynamic 'on-and-off' chelating effect for the metal center.[21,22]

Heteroditopic ligands of hemilabile character that combine strong electron donors and weak donor functions linked by a flexible backbone, as for example Ph$_2$P(CH$_2$)$_n$Z (Z = OR, NR$_2$, SR),[23] should allow a dynamic interaction with the metal center, and/or stabilization of polar intermediates in catalytic applications, exerting some directing effect. We have discovered that cationic rhodium(I) complexes containing these hemilabile phosphine ligands, [Rh(diene){Ph$_2$P(CH$_2$)$_n$Z}]$^+$, are efficient catalysts precursors for the stereoregular polymerization of substituted PAs. Remarkably high number-average molecular weight stereoregular polyphenylacetylenes of up to 1 750 000 have been obtained and an active role of the hemilabile ligand in the generation of intermediate alkynyl species has been identified by spectroscopic means under stoichiometric and catalytic conditions. We report herein the effect of the donor ability of the hemilabile fragment

(-OMe, -NMe$_2$ or -SMe), the length of the flexible carbon chain (n) and the nature of the diene ligand on the PA polymerization activity and PPA properties.

Results

Synthesis of Cationic Rhodium Complexes Containing Functionalized Phosphine Ligands [Rh(diene){Ph$_2$P(CH$_2$)$_n$Z}][BF$_4$] (1–7). We have prepared a series of mononuclear cationic rhodium complexes containing functionalized P,O-, P,S-, or P,N- phosphine ligands,[23] [Rh(diene){Ph$_2$P(CH$_2$)$_n$Z}][BF$_4$], as catalyst precursors for PA polymerization. The complexes [Rh(cod){Ph$_2$P(CH$_2$)$_2$Z}][BF$_4$] (n = 2, Z = OMe (**1**), SMe (**2**), NMe$_2$ (**3**)), [Rh(cod){Ph$_2$P(CH$_2$)$_3$OMe}][BF$_4$] (**4**) and [Rh(diene){Ph$_2$P(CH$_2$)$_3$NMe$_2$}][BF$_4$] (diene = cod (**5**), tfb (**6**), nbd (**7**)) have been synthesized (Chart 1).

diene = cod

1   Z = OMe
2   Z = SMe
3   Z = NMe$_2$

4   diene = cod, Z = OMe
5   diene = cod, Z = NMe$_2$
6   diene = tfb,   Z = NMe$_2$
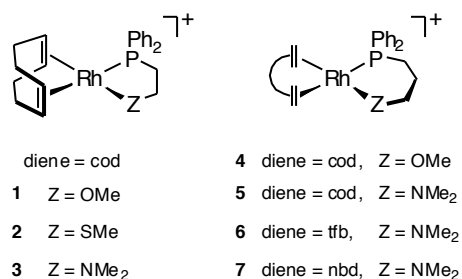**7**   diene = nbd, Z = NMe$_2$

Chart 1

The cationic complexes [Rh(diene){Ph$_2$P(CH$_2$)$_n$Z}]$^+$ are accessible by two different methods starting from the dinuclear complexes [Rh(μ-Cl)(diene)]$_2$ through the cationic solvate species [Rh(diene)(solvent)$_2$]$^+$ (solvent = tetrahydrofuran or acetone) or the neutral species [RhCl(diene){Ph$_2$P(CH$_2$)$_n$Z}] (Scheme 1).

The complexes [Rh(diene){Ph$_2$P(CH$_2$)$_n$Z}][BF$_4$] (**1–7**) behave as 1:1 electrolytes in acetone and have been fully characterized by elemental analysis, mass spectra and multinuclear NMR spectroscopy. The spectroscopic data are in agreement with the expected square planar geometry of the complexes that are determined by the coordination of a diene ligand (cod, nbd or tfb) and a chelating Ph$_2$P(CH$_2$)$_n$Z ligand. Thus, two broad resonances (1:1 ratio) were observed for the =CH protons of the diene ligand in the ^{1}H NMR spectra whereas that the ^{13}C{^{1}H} NMR spectra features two well defined resonances, a doublet of doublets ($J_{C-Rh} \approx 10$ and $J_{C-P} \approx 7$ Hz) and a doublet ($J_{C-Rh} \approx$

12–15 Hz), for the olefinic carbon atoms *trans* to the P donor atom and the heteroatom (Z), respectively. On the other hand, the $^{31}P\{^1H\}$ NMR spectra of the complexes features the expected doublet with a J_{P-Rh} in the range 150–170 Hz.
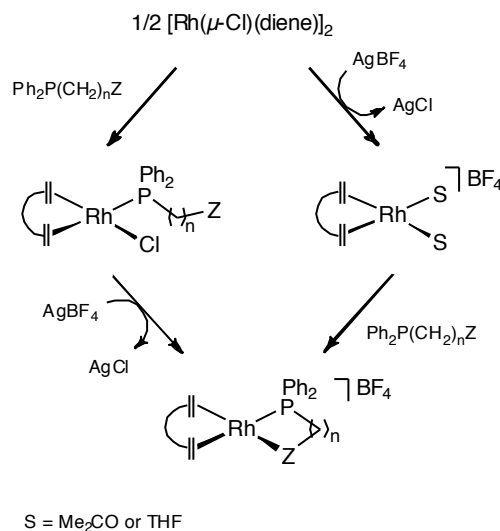
Scheme 1

The crystal structures of complexes **5** and **6** have been determined by X-ray diffraction methods and confirm the proposed ligand arrangement. The molecular structures of these compounds are shown in Figures 1 and 2.
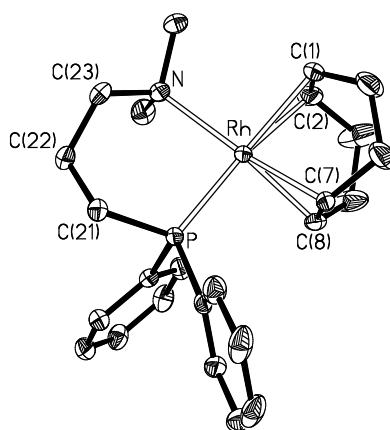

Figure 1. Molecular structure of the cation of $[Rh(cod)\{Ph_2P(CH_2)_3NMe_2\}]BF_4$ (**5**). Selected bond distances (Å) and angles (deg): Rh–P 2.2872(8), Rh–N 2.262(3), Rh–C(1) 2.261(3), Rh–C(2) 2.258(3), Rh–C(7) 2.142(3), Rh–C(8) 2.133(3); P–Rh–N 90.24(7); M(1)[a]–Rh–M(2)[a] 84.8(1). [a] M(1) and M(2) represent the midpoints of the olefinic double bonds C(1)–C(2) and C(7)–C(8) bonds, respectively.
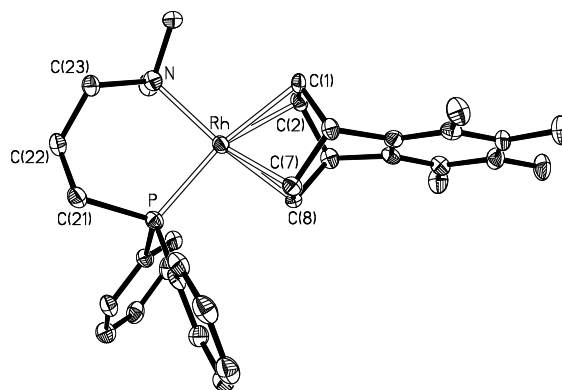
Figure 2. Molecular structure of the cation of $[Rh(tfb)\{Ph_2P(CH_2)_3NMe_2\}]BF_4$ (**6**). Selected bond distances (Å) and angles (deg): Rh–P 2.2722(138), Rh–N 2.190(4), Rh–C(1) 2.262(5), Rh–C(2) 2.240(5), Rh–C(7) 2.104(5), Rh–C(8) 2.112(4); P–Rh–N 92.23(11); M(1)[a]–Rh–M(2)[a] 69.2(1). [a] M(1) and M(2) represent the midpoints of the olefinic double bonds C(1)–C(2) and C(7)–C(8) bonds, respectively.

The most remarkable molecular parameter differentiating both molecules involves the Rh–N bond distance, 2.262(3) in **5** *vs*. 2.190(4) Å in **6**. Most likely, the electron withdrawing character of the tfb diene, compared to that of cod, reinforces the σ-bonding Rh–N interaction in **6**; associated to this modification there is also a significant shortening of the Rh–C bond distances *trans* to the amino nitrogen (1.988(4) (**6**) vs. 2.021(2) Å (**5**)). Both 6-membered metallacycles, Rh–P–C(1)–C(2)–C(3)–N, show analogous twisted conformations with similar puckering amplitudes [0.629 (**5**) *vs*. 0.587 Å (**6**)].

Polymerization of PA by $[Rh(cod)\{Ph_2P(CH_2)_nZ\}][BF_4]$ (1–5) catalysts. Polymerization of PA with catalyst precursors **1–5**, containing cod as diene ligand, was carried out in THF or in toluene saturated with water (wet toluene, in order to fully solubilize the catalyst precursors) at 30 ºC using a monomer-to-rhodium ratio $[PA]_0/[Rh]$ of 100, without any co-catalyst. In general, the reactions were faster in wet toluene than in THF, except for catalyst precursor **2**, as can be inferred from the reaction time required to get conversions over 90% (Table 1). The highest catalytic activities were

obtained with catalysts **1** and **5** that provided PPA quantitatively in one hour. In fact, conversions of ca. 70 % were observed after 1 min. Among **1–4**, catalyst **1** afforded the polymer with the highest number average molecular weight, M_n of 86 000, and the narrowest molecular weight distribution, M_w/M_n of 1.54, in wet toluene. However, the PPA obtained with catalysts **1** and **2** in THF displayed a bimodal molecular weight distribution. In sharp contrast, catalyst **5** gave a bimodal profile in wet toluene but, interestingly, a high molecular weight PPA, M_n = 160 000 with M_w/M_n of 1.62, was attained in THF. In sharp contrast, catalyst **5** gave a bimodal profile in wet toluene but, interestingly, a high molecular weight PPA, M_n = 160 000 with M_w/M_n of 1.62, was attained in THF. The polymerization in other polar solvents such as diethyl ether, acetone or methanol, was slower and also afforded PPA with a unimodal GPC profile but with much lower molecular weights (M_n = 25 000–33 000) and wide molecular weight distribution (M_w/M_n > 2.4) (see Supporting Information). Thus, the best catalytic performance of **5**, both in terms of activity and PPA properties, was achieved in THF where the polymerization proceeds homogeneously. The high M_n of the polymer achieved with catalyst **5** and the moderate polydispersity ratio suggest that the rate of chain-growth is faster than the initiation and termination steps, which is compatible with the low initiation efficiency, IE = 6%.[24]

The formation of PPA with a bimodal molecular weight distribution was evident, in some cases, in the form of a low or high MW shoulder on the side of the main distribution. The interpretation of the bimodality seen is complicated by the time- and solvent-dependent conformational or aggregational behavior of high cis-PPA in solution[25] during either polymer synthesis or possibly subsequent SEC analysis.[26] While it is tempting to interpret the bimodality observed to e.g. different catalyst species propagating independently, an equally valid interpretation involves different physical states for the polymer chain (e.g. extended vs. random coil, soluble vs. suspended) during growth with slow interconversion relative to propagation. Our data do not allow one to distinguish between these possibilities.

Table 1. Polymerization of PA Catalyzed by [Rh(diene){Ph$_2$P(CH$_2$)$_n$Z}]BF$_4$ (**1–7**).[a]

| | | | | Polymer | |
Catalyst	Solvent	Time (min)	Yield (%)[b]	M_n[c]	M_w/M_n[c]
1	Wet toluene	60	99	86 000	1.54
	THF	80	98	165 000 (28%)	1.13
				24 000 (72%)	2.07
2	Wet toluene	1120	70	16 000	2.67
	THF	120	93	76 000	1.66
3	Wet toluene	230	95	82 000	1.76
	THF	1120	84	24 000	2.87
4	Wet toluene	90	99	77 000	1.55
	THF	210	94	16 000 (23%)	1.12
				19 000 (77%)	2.37
5	Wet toluene	60	97	168 000 (55%)	1.16
				27 000 (45%)	1.88
	THF	86	93	160 000	1.62
6	THF	45	97	970 000	1.70
7	THF	30	100	1 420 000	1.53

[a] T = 30 ºC, [PA]$_0$ = 0.25 M, [PA]$_0$/[Rh] = 100. Wet toluene (toluene saturated in water) [b] Determined by GC (octane as internal standard). [c] Determined by GPC (THF, PSt).

Polymerization of PA by [Rh(diene){Ph$_2$P(CH$_2$)$_3$NMe$_2$}][BF$_4$] (5–7) catalysts. The efficiency of the catalyst precursor based on the ligand Ph$_2$P(CH$_2$)$_3$NMe$_2$ prompted us to develop new catalysts based on this hemilabile ligand and to study the influence of the reaction conditions on the catalysts achievement and polymer properties. In particular, the influence of the diene ligand and the effect of the temperature, catalyst precursor loading and the addition of water or an external base such as, DMAP (4-dimethylaminipyridine), on the polymerization of PA in THF have been investigated in detail.

1. The influence of the diene ligand. The influence of the diene ligand on the polymerization of PA has been studied by using the complexes [Rh(diene){Ph$_2$P(CH$_2$)$_3$NMe$_2$}][BF$_4$] (diene = cod (**5**), tfb (**6**), nbd (**7**)) as catalysts. Polymerization of PA with catalysts **5–7** in THF at 30 ºC for 1 min at

a $[PA]_0/[Rh]$ ratio of 100 gave the following conversions: **5** (cod) 45%, **7** (nbd) 67%, **6** (tfb) 76%.

Thus, a steady improvement on the activity was observed when increasing the π-acidity of the

diene ligand in full agreement with the results reported by Masuda *et al*.[27] However, the monitoring

of the time-conversion curves showed that catalyst **7** (nbd) exhibited a superior performance with

time than **6** (tfb) with times for a conversion >95% of 22 and 45 min, respectively. Interestingly,

the PPA obtained with catalysts **6** (tfb) and **7** (nbd) displayed an outstandingly high number-

average molecular weights (M_n) of 970 000 ($IE = 1\%$) and ($IE = 0.7\%$) 1 420 000 (Figure 3),

respectively, with moderate polydispersity indexes (M_w/M_n) of 1.70 and 1.53, respectively. Thus,

catalyst **7** (nbd) provided the PPA with the highest M_n and narrowest molecular weight distribution.

The weight-average molecular weight ($M_w = 2\ 170\ 000$) is, to the best of our knowledge, one of the

largest ever reported using rhodium catalysts. For comparison, catalyst $[Rh(nbd)(dbn)_2]^+$ (dbn =

1,5-diazabicyco[4.3.0]non-5-en) gave a PPA with a M_w of 1 745 060.[14b]

Legend:
- Mn = 1 420 000; Mw/Mn = 1.53
- Mn = 970 000; Mw/Mn = 1.70
- Mn = 160 000; Mw/Mn = 1.62

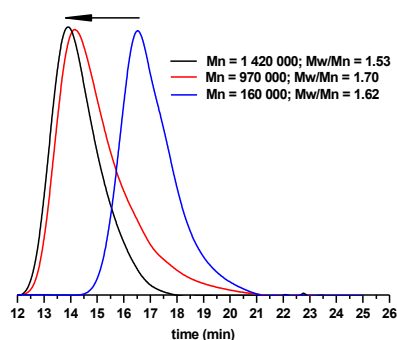x-axis: 12 13 14 15 16 17 18 19 20 21 22 23 24 25 26 time (min)

Figure 3. GPC traces of PPAs obtained by polymerization of PA catalyzed by

$[Rh(diene)\{Ph_2P(CH_2)_3NMe_2\}]BF_4$ (blue line, cod **5**; red line, tfb **6**; black line, nbd **7**) in THF, 30

ºC, $[PA]_0 = 0.25$ M, $[PA]_0/[Rh] = 100$, at 100 % conversion.

2. Effect of Temperature. The effect of the temperature on the polymerization of PA by **7**, the

most efficient catalyst, was examined in the range 0–60 ºC. As can be observed in Figure 4, at

lower temperature higher M_w PPA with a narrower molecular weight distribution was formed. The

polymerization of PA by **7** at 0 ºC under more diluted conditions, in order to avoid the precipitation

of PPA ($[Rh] = 1.25$ mM, $[PA]_0/[Rh] = 100$), went to completion in 30 min. The PPA produced

under these conditions showed a M_n of 1 760 000 and M_w/M_n of 1.36. On the other hand, the PPA obtained when the polymerization was carried out at 60 °C showed a bimodal GPC profile.
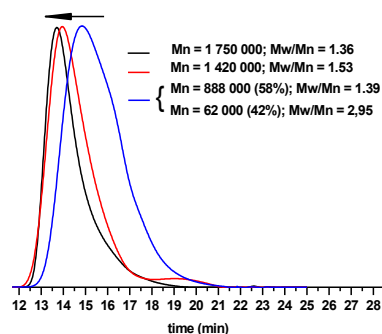

Figure 4. GPC traces of PPAs obtained by polymerization of PA catalyzed by [Rh(nbd){Ph$_2$P(CH$_2$)$_3$NMe$_2$}]BF$_4$ (**7**) at different temperatures in THF, [PA]$_0$ = 0.25 M, [PA]$_0$/[Rh] = 100 (red line, 30 °C, blue line, 60 °C), [PA]$_0$ = 0.125 M (black line, 0 °C), at 100 % conversion.

3. Effect of PA/Rhodium Ratio. The effect of increasing the [PA]$_0$/[Rh] ratio in the polymerization of PA has been studied with catalysts **6** (tfb) and **7** (nbd) giving similar results. The time course of polymerization with **7** at different [PA]$_0$/[Rh] ratios (16000–100) was monitored by GC and it is shown in Figure 5a. As expected, the time required for the quantitative consumption of PA increased on increasing the PA concentration at the same [Rh]. However, the polymerization is very fast up to the 50% conversion even using a [PA]$_0$/[Rh] ratio as high as 16000 although, unfortunately, the polymerization stops after 100 min at 70% conversion.
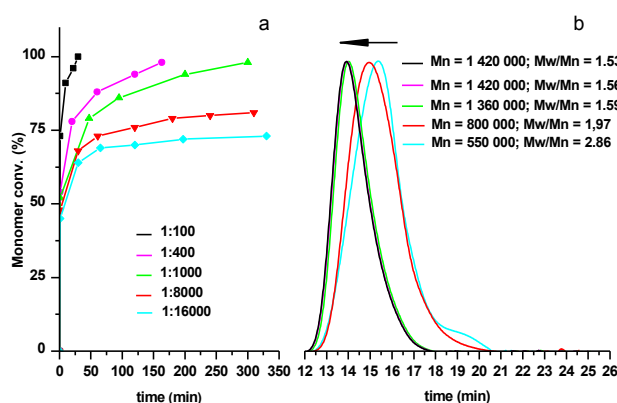

Figure 5. Polymerization of PA with [Rh(nbd){Ph$_2$P(CH$_2$)$_3$NMe$_2$}]BF$_4$ (**7**) at different [PA]$_0$/[Rh] ratios: THF, 30 °C, [Rh] = 2.5 mM (**7**). a) Time-conversion curves determined by GC; b) GPC traces.

The GPC traces of PPAs obtained by polymerization of PA with **7** at different $[PA]_0/[Rh]$ ratios after 2 hours are shown in Figure 5b. The increase of the $[PA]_0/[Rh]$ ratio up to 4000 has no a significant influence on the molecular weight of the polymer which smoothly increase up to $M_n = 1\,220\,000$ with M_w/M_n indexes in the range of 1.59–1.74. However, a dramatic drop in M_n and wider molecular weight distributions were observed in the PPA obtained at $[PA]_0/[Rh]$ ratios higher than 8000.

4. Effect of Water. The addition of water to the reaction media has a positive influence on the catalytic activity. The effect of water in the polymerization of PA has been studied in THF at 30 ºC using $[Rh(nbd)\{Ph_2P(CH_2)_3NMe_2\}]BF_4$ (**7**) as catalyst ($[Rh] = 0.62$ mM, $[PA]_0/[Rh] = 400$). The attained conversions after 1 min at $[H_2O]/[Rh]$ ratios of 0, 200 and 400 were 54 %, 60 % and 75%, respectively, showing a steady improvement of the catalytic activity when increasing the water concentration in the reaction media. However, the GPC profiles of PPAs obtained under these conditions at 100 % conversion (Figure 6) showed an adverse effect both on M_n and M_w/M_n.
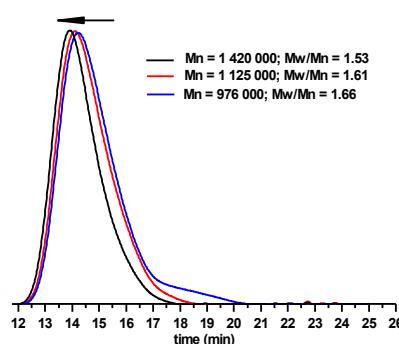

Figure 6. GPC trace of PPAs obtained by polymerization of PA with $[Rh(nbd)\{Ph_2P(CH_2)_3NMe_2\}]BF_4$ (**7**) in THF in the presence of water, 30 ºC, $[PA]_0 = 0.25$ M, $[PA]_0/[Rh] = 400$, at 100 % conversion. $[H_2O]/[Rh] = 0$, black line; 200, red line; 400, blue line.

5. Effect of Base (DMAP). Noyori *et al.*[16] have described the positive effect of the addition of an external base (DMAP, 4-(dimethylamino)pyridine) on the polydispersitiy index of PPA. The polymerization of PA with **7** (nbd) in THF at 30 ºC in the presence of DMAP ($[Rh] = 2.5$ mM, $[PA]_0/[Rh] = 100$, $[DMAP] = 2.5$ mM) at 100 % conversion gave, unexpectedly, a PPA with lower molecular weight, $M_n = 233\,000$ (*IE* = 4.3 %), and a narrower molecular weight distribution

($M_w/M_n = 1.34$) than that obtained without DMAP. The polymerization of PA with **6** (tfb) under the same conditions gave even lower molecular weight PPA ($M_n = 106\,000$, $IE = 10\%$) with a M_w/M_n of 1.20.

In order to study the living character of the polymerization by the system **6**/DMAP a multistage polymerization experiment has been carried out. Three PA feeds were supplied at intervals of 30 min to ensure for the complete consumption of PA after each monomer feed (monitored by GC). The obtained time-conversion curve (Figure 7a) evidenced the positive effect of DMAP on the catalytic activity since the reaction speeds up by a factor of 10. The GPC traces of PPAs obtained after each stage in the multistage polymerization (Figure 7b) showed an increase of the M_n in direct proportion to the monomer consumption both after the second ($M_n = 196\,000$) and third feeds ($M_n = 293\,000$). The growing of the polymer chain is followed by a fairly increase in the polydispersity index up to 1.38. The initiation efficiencies after each monomer addition remains constant (*IE ca* 10%) which suggest that initiation is the rate determining step in the presence of DMAP. This behaviour contrast with the observed in the multistage polymerization of PA carried out with **6** (tfb) without DMAP under the same conditions that gave the following results: 1st load ($M_n = 970\,000$, $M_w/M_n = 1.79$), 2nd load ($M_n = 1\,130\,000$, $M_w/M_n = 1.56$), 3rd load ($M_n = 850\,000$, $M_w/M_n = 1.59$).
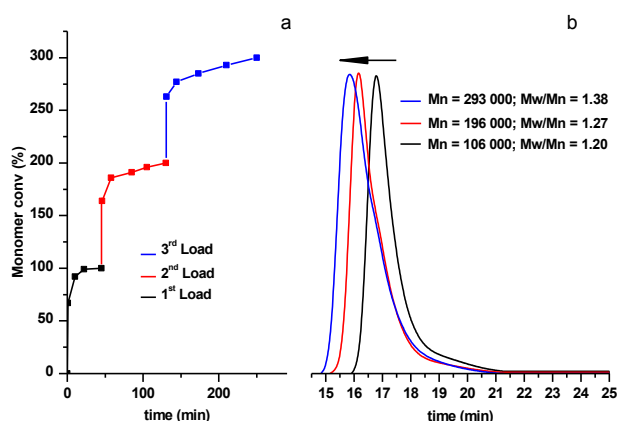

Figure 7. Multistage polymerization of PA catalyzed by [Rh(tfb){Ph_2P(CH_2)_3NMe_2}]BF_4 (**6**) in the presence of DMAP: THF, 30 ºC, [PA]_0 = 0.25 M, [PA]_0/[Rh] = 100, [DMAP] = 2.5 mM. a)

Monomer conversion *vs* time (PA feeds were supplied at 100 % of conversion after each load); b) GPC traces of PPAs obtained after each stage in the multistage polymerization.

The quasi-living nature of the polymerization reaction[28] by the system **6**/DMAP has allowed the synthesis of an AB type block copolymer from two different PAs. Thus, the reaction of PPA with an M_n of 106 000 and M_w/M_n of 1.20 with *p*-methoxyphenylacetylene (MeOPA, 100 molar equiv) in THF gave a PPA-MeOPA block copolymer with M_n of 184 000 and an M_w/M_n of 1.44. The ^{1}H NMR spectrum of this copolymer features two sharp singlets for the vinylic protons of the phenyl and p-methoxyphenyl copolymer units at δ 5.85 and 5.77 ppm, respectively (Figure 8b).
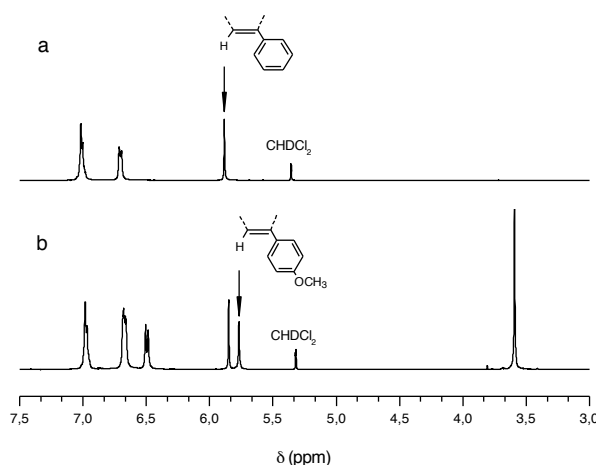

Figure 8. ^{1}H NMR spectrum in CDCl$_3$ at 298 K of a) PPA; b) PPA-MeOPPA block copolymer obtained with the system **6**/DMAP.

Polyphenylacetylene properties. Stereoregular PPA can present four stereoisomers in terms of the configuration of the C=C bond and the conformation of the C-C single bond of the polymer backbone. However, rhodium-catalyzed polymerization of monosubstituted acetylenes usually produces stereoregular polymers with a head-to-tail *cis-transoidal* main chain structure.[11–19]

The PPA polymers obtained with catalysts **1**–**7** were isolated as soluble yellow-orange solids with a plastic-like appearance. The sharp signal at δ 5.82 ppm (vinyl protons) in the ^{1}H NMR spectra (Figure 8a) and the set of six signals observed in the ^{13}C{^{1}H} NMR spectra in CDCl$_3$ are

indicative of a high stereoregular sequence in the polymers.[29] In fact, the *cis*-content of the

polymers determined by NMR was quantified to be superior to 99%.[30]

The thermal properties of the polymers have been studied by thermogravimetry analysis (TGA)

and differential scanning calorimetry (DSC). Figure 9a shows a representative TGA curve of a

sample of the polymer obtained with catalyst **6** (tfb). No thermal decomposition was observed at

temperatures below 200 ºC and only a slight weight lose (aprox. 4%) was detected. A sharp weight

lose corresponding to thermal descomposition was observed above 250 ºC (onset on the

decomposition step), what is in accordance with the TGA curves of other polyphenylacetylenes

analyzed.[31] The DSC curves for the same polymer sample are illustrated in Figure 9b (three

consecutive heating/cooling processes at 10ºC/min were recorded). An obvious exothermic peak

was detected at around 150 ºC in the first heating run. As no thermal decomposition was observed

in the TGA curve at this temperature range, this irreversible exothermic peak could be assigned to

exothermic polymer reactions such as *cis*↔*trans* isomerization or the crosslinking of polymer

chains. No peak or baseline jumps were observed in the following scans either in the heating or
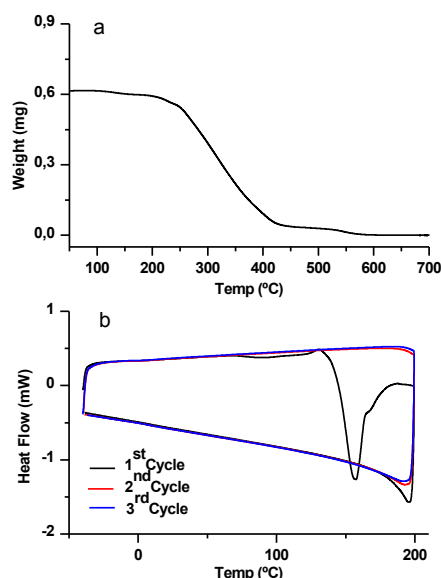
cooling processes.

Figure 9. Thermal analysis of PPA films. a) TGA; b) DSC scans of three consecutive

heating/cooling processes at 10 ºC/min.

In order to study the origin of the exothermic peak, films of PPA were analyzed by FT-IR before and after heating at 150ºC (corresponding to the thermal event on DSC). The peak observed in the DSC is not due to cross-linking of the double carbon-carbon bonds because there is no modification on the main features of the absorptions at 1494–1440 cm^{-1} and 1605 cm^{-1}, assigned to stretching vibrations of aromatic rings and polyconjugated trisubstituted carbon-carbon double bonds, respectively.[32] However, the FT-IR spectrum of the PPA after heating showed a new absorption at 1265 cm^{-1} (Figure 10). This band has been attributed to the vibrational C-C bond stretching in the *trans* chain, coupled with that of the C-H bond in the C=CH group.[33] This observation strongly supports a thermal-induced *cis↔trans* isomerization process.[34]

The *cis* content of PPA can also be estimated from the intensity of the 740 and 760 cm^{-1} bands in the FT-IR spectrum.[35] As the absorption at 740 cm^{-1} is representative of the *cis* content in the polymer, and the absorption at 760 cm^{-1} is assigned to C-H out-of-plane deformations of phenyl rings, the ratio between intensities of these two absorptions (I_{740}/I_{760}) is a measurement of the *cis* content that, in our case, correlates with the percentage determined by NMR. The significant reduction in the intensity of the 740 cm^{-1} band after heating of a PPA film at 150 ºC for 30 min (Figure 10) futher support the change in the geometrical structure of the polymer main chain upon heating.
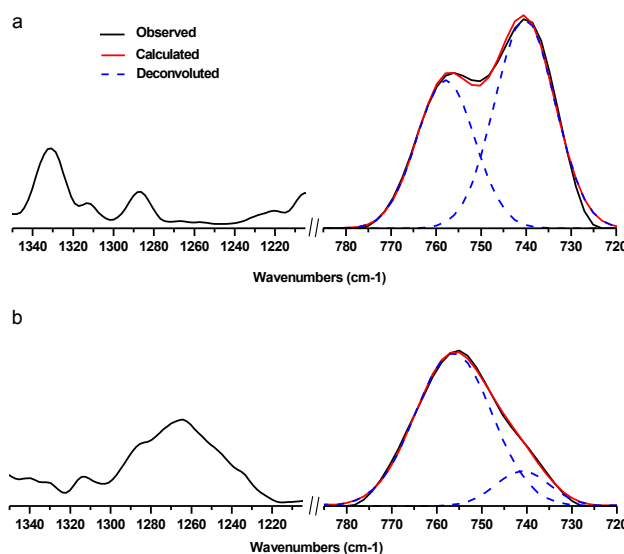
Figure 10. FT-IR spectra of PPPAs films in the 1350 – 1200, and 720 – 780 cm^{-1} regions. Black lines, observed spectra. Red lines, simulated spectra as the sum of the two deconvoluted peaks, blue lines, at 740 and 760 cm^{-1}. (a) Fresh polymer sample; (b) Polymer after heating at 150 °C for 30 min.

NMR spectroscopic studies on the polymerization mechanism. The evolution of the catalytic precursor [Rh(cod){Ph$_2$P(CH$_2$)$_3$NMe$_2$}][BF$_4$] (**5**) in the presence of PA has been investigated by NMR spectroscopy. A yellow solution of **5** in CD$_2$Cl$_2$ was treated with PA, [PA]/[**5**] molar ratio of 10, at -78 °C and then the temperature was allowed to warm up to 25 °C to give immediately a red solution. The monitoring of the reaction by ^{31}P{^{1}H} NMR showed the presence of **5** at δ 17.69 ppm ($J_{\text{P-Rh}}$ = 155.7 Hz) and evidenced the formation of a new species at δ 23.29 ppm ($J_{\text{P-Rh}}$ = 158.3 Hz) after 1 min (Figure 11). The concentration of this species diminished along time and a new species, in a fairly minor proportion, at δ 18.01 ppm ($J_{\text{P-Rh}}$ = 143.7 Hz) was noticed at approximately 3 min. Interestingly, the disappearance of both species and the recovery of **5** was observed at longer reaction times. An additional feed of PA gave the same ^{31}P{^{1}H} NMR spectra series and only compound **5** was observed at the end of the polymerization reaction.

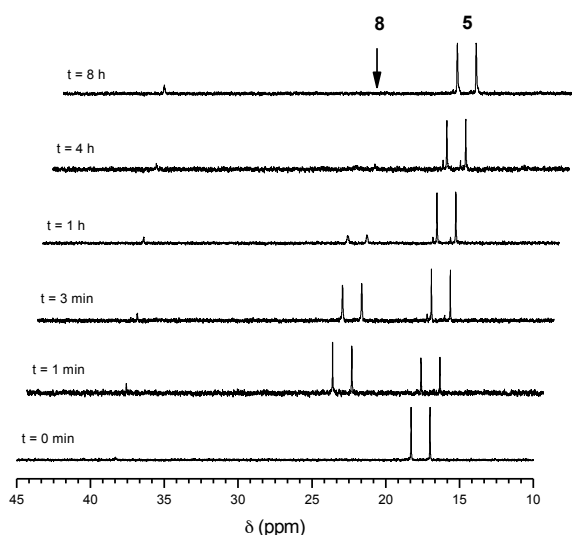**Figure 11.** ^{31}P{^{1}H} NMR spectra (CD$_2$Cl$_2$, 298 K) at selected times for the reaction of [Rh(cod){Ph$_2$P(CH$_2$)$_3$NMe$_2$}][BF$_4$] (**5**) (0.014 mmol, 0.028 M) with PA (0.14 mmol, 0.28 M).

The species observed at δ 23.29 ppm was quantitatively formed when the reaction was conducted in THF-d_8 or in CD_2Cl_2 at -30 °C using a [PA]/[**5**] molar ratio of 20, and has been characterized as the square-planar alkynyl complex [Rh(C≡C-Ph)(cod){Ph$_2$P(CH$_2$)$_3$NHMe$_2$}]BF$_4$ (**8**) (Scheme 2). The $^{13}C\{^1H\}$ NMR spectrum of **8** shows two resonances at δ 122.18 (dd, $J_{C-Rh} = 48.7$, $J_{CP} = 21.8$ Hz) and 120.30 ppm (d, $J_{C-Rh} = 17.9$ Hz) attributable to the C$_\alpha$ and C$_\beta$ of the alkynyl moiety, respectively. In addition, the ^1H NMR spectrum features a broad signal at δ 8.54 ppm that corresponds to the acid proton of -NMe$_2$H fragment resulting from the deprotonation of PA. Unfortunately, the species at δ 18.01 ppm in the $^{31}P\{^1H\}$ NMR spectrum could not be identified due to its small proportion in the reaction mixture, although it can be tentatively assigned to the active propagating species or to an alkynyl-η^2-alkyne intermediate species. Catalyst **6** (tfb) behaves similarly under the same experimental conditions and a species related to **8** has been observed at δ 26.68 ppm (d, $J_{C-Rh} = 172.0$ Hz) although at lower concentration in agreement with the higher activity of this catalytic system.
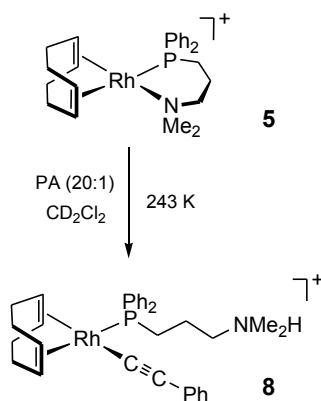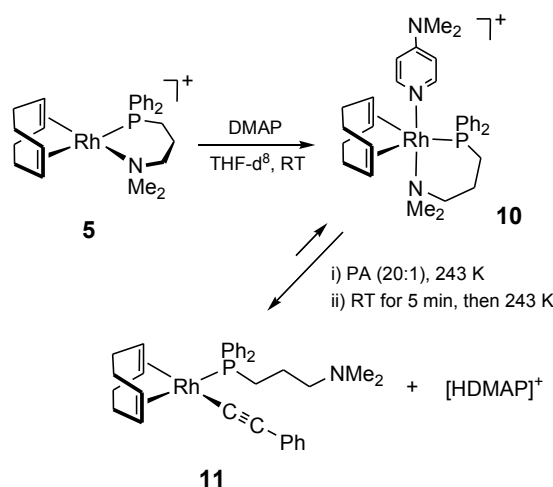

Scheme 2

In order to ascertain the role of DMAP in this catalytic system the reactivity of compounds **5** (cod) and **6** (tfb) with DMAP was studied by NMR. The $^{31}P\{^1H\}$ NMR spectrum of a CD_2Cl_2 solution of **6** after addition of 1 molar-equiv of DMAP at RT showed a broad resonance at δ 22.34 ppm that was resolved into a doublet at δ 24.37 ppm ($J_{P-Rh} = 176.7$ Hz) at 213 K. The ^1H NMR spectrum at 213 K evidenced the coordination of DMAP to the rhodium center and the formation of the species [Rh(tfb){Ph$_2$P(CH$_2$)$_3$NMe$_2$}(DMAP)]$^+$ (**9**). Compound **9** is fluxional and shows a broad

resonance for the =CH protons of the tfb ligand which suggest a dynamic pentacoordinated structure. Similarly, compound **5** reacted with DMAP to give the species [Rh(cod){Ph$_2$P(CH$_2$)$_3$NMe$_2$}(DMAP)]$^+$ (**10**) that also exhibits a fluxional behavior. However, the spectroscopic data al 253 K suggest a square planar structure with an uncoordinated NMe$_2$ fragment (Scheme 3).

The reaction of **10** with PA was monitored by NMR. The addition of 20 molar-equiv of PA to a solution of **10**, generated in situ from **5**, in THF-d_8 at -78 ºC following of stirring at RT for 5 min. gave a red solution. The ^{31}P{^{1}H} NMR spectrum at 243 K showed the presence of two new species at δ 25.57 ($J_{\text{P-Rh}}$ = 158.3 Hz) and 13.59 ppm ($J_{\text{P-Rh}}$ = 108.3 Hz) (< 10%) along with **10**. The main species at δ 25.57 ppm has been characterized as the neutral square-planar complex [Rh(C≡C-Ph)(cod){Ph$_2$P(CH$_2$)$_3$NMe$_2$}] (**11**) (Scheme 3). In addition, the cation [HDMAP]$^+$ resulting from the deprotonation of PA, was also detected by NMR.[36] In contrast to **10**, compound **11** is rigid and shows the expected pattern of resonances for the alkynyl ligand at δ 119.47 (dd, $J_{\text{C-Rh}}$ = 43.4, $J_{\text{C-P}}$ = 23.4 Hz) and 115.51 ppm (d, $J_{\text{C-Rh}}$ = 13.3 Hz) in the ^{13}C{^{1}H} NMR spectrum. On the other hand, the resonance of the –NMe$_2$ group was observed at δ 42.64 ppm, 9 ppm upfield compared with **5**, support the presence of an uncoordinated the -NMe$_2$ fragment and rules out a possible pentacoordinated structure for **11**.

Scheme 3

Discussion

It is well established that polymerization of substituted phenylacetylenes catalyzed by rhodium complexes proceeds through an 2,1-insertion mechanism that usually produce stereoregular polymers with a a *cis-transoidal* structure,[37] which is in good agreement with the theoretical calculations based on model compounds.[38] On the other hand, it is thought that flexible ligands could enhance insertion reactions; in fact, Pollack *et al*.[39] have shown that the catalytic performance of diphosphine-palladium(II) complexes in PA polymerization is higher with diphosphines having a flexible backbone. In accordance with this, the flexibility imparted by the hemilabile functionalized phosphine ligands, that should favor the insertion process, could be probably responsible for the high catalytic activity of the complexes $[Rh(diene)\{Ph_2P(CH_2)_nZ\}]^+$. However, there is not an obvious correlation between the length of the flexible chain (n) or the donor group (Z), and the catalytic activity or the molecular weight of the obtained polymers (Table 1). In fact, the best catalyst precursors in the cod series turn out to be the complexes $[Rh(cod)\{Ph_2P(CH_2)_2OMe\}]^+$ (**1**) and $[Rh(cod)\{Ph_2P(CH_2)_3NMe_2\}]^+$ (**5**) that have very different functionalized phosphine ligands.

The solvent plays a decisive role in the polymerization reactions.[40,41] The catalytic activity of **5** is superior in toluene or in toluene/polar solvent mixtures but the polymers show bimodal molecular weight distributions. In contrast, the catalytic activity decreases when increasing the dielectric constant of the solvent but, interestingly, the polymers display unimodal GPC traces. THF presents an adequate balance between both factors since unimodal polymers were attained with good activities. It is worth mentioning that the same solvent effect on the catalytic activity has been observed in several systems based on rhodium-vinyl complexes.[18]

Diene ligands strongly influence the catalytic activity in rhodium polymerization catalysts. In general, rhodium complexes with nbd as diene ligand were found to be more active than those of cod,[42] although there are remarkable exceptions.[40,43] In addition, Masuda *et al*. have reported that complexes $[Rh(\mu\text{-}Cl)(tfb)]_2$ or $[Rh(\mu\text{-}Cl)(tcb)]_2$ (tcb = tetrachlorobenzobarralene) are more active that the analogue nbd complexes.[27] This fact has been explained in terms of the different π-acidity of the diene ligands. Thus, the high π-acidity of tfb results in the reduction of the electronic density

at the rhodium center enhancing its electrophilic character that, in turn, facilitates the coordination of the monomer. This reactivity pattern has also been found in the complexes $[Rh(diene)\{Ph_2P(CH_2)_3NMe_2\}]^+$ since **6** (tfb) and **7** (nbd) are far more active than **5** (cod). Noteworthy, both complexes gave PPA with huge number-average molecular weights (M_n) of 970 000 (**6**, tfb) and 1 420 000 (**7**, nbd) under the same experimental conditions used for **5** (cod). Futhermore, the addition of DMAP resulted in a dramatic drop in the PPA molecular weight, 106 000 (**6**, tfb) and 233 000 (**7**, nbd), as a consequence of the increase of initiation efficiency. In addition, the PPA obtained with the system **6**/DMAP showed a narrow molecular weight distribution M_w/M_n of 1.20 and multistage polymerization experiments have demonstrated the quasi-living nature of the reaction under these conditions.

The monitoring of PA polymerization by $^{31}P\{^1H\}$ NMR at RT using **5** as catalyst has allowed the identification of the cationic compound $[Rh(C\equiv C\text{-}Ph)(cod)\{Ph_2P(CH_2)_3NHMe_2\}]^+$ (**8**). This unusual η^1-alkynyl complex, which has been quantitatively formed from **5** and PA at low temperature, probably results from the intramolecular proton transfer from a η^2-alkyne ligand to the hemilabile ligand.[44] On the other hand, the formation of the neutral alkynyl complex $[Rh(C\equiv C\text{-}Ph)(cod)\{Ph_2P(CH_2)_3NMe_2\}]$ (**11**) from **5**, DMAP and PA strongly suggests that role of the DMAP in the initiation step is also the deprotonation of a η^2-alkyne ligand. In this case, the DMAP behaves as an external base although probably the coordination to the metal center is required for the proton transfer and formation of $[HDMAP]^+$, as was evidenced by the formation of $[Rh(cod)\{Ph_2P(CH_2)_3NMe_2\}(DMAP)]^+$ (**10**) from **5** and DMAP (Scheme 3). On the light of the calculated initiation efficiencies in the catalytic tests with and without DMAP, it becomes evident that the proton transfer to DMAP is more effective. It is noticeable that catalytic systems based on rhodium complexes are, in general, tolerant with water.[40–42] We have found that the addition of water has a positive effect on the catalytic activity (Figure 6) which can be rationalized in terms of a more facile proton transfer process but, at the same time, the termination step is also favored multiplying the number of different polymeric species giving broader GPC profiles.

The propagating step in PA polymerization has been proposed to occur through two very different mechanisms: a metathesis mechanism via metal-carbene species, and an insertion mechanism via a metal-vinyl complex.[45] However, elegant isotope labeling studies by Noyori *et al*. have demonstrated that rhodium PA polymerization proceeds via a *cis*-insertion mechanism (2,1-regioselectivity) in rhodium-vinyl intermediates.[16c,46] Noyori *et al*. have also studied the initiation step in the catalytic system [Rh(C≡C-Ph)(nbd)(PPh$_3$)$_2$]/DMAP, the no incorporation of isotope-labeled alkynyl fragment in the polymer ruled out the direct insertion of PA into the rhodium-alkynyl bond as initiation mechanism. On the other hand, the detection of 1,4-diphenylbuta-1,3-diyne, probably formed by oxidation addition of PA to a square-planar alkynyl compound followed by reduction elimination, strongly suggest the participation of a rhodium-hydride species in the generation of the active vinyl intermediates. Furthermore, the diyne is also involved into the deactivation of the catalyst via the formation of a rhodacyclopentadiene complex, which further support the participation of rhodium-hydride species.[16c]

The formation of the alkynyl complex **8** from **5** and PA under catalytic conditions strongly suggests that the alkynyl ligand in **8** could have an active role in the initiation process. Although a possible initiation mechanism involving the oxidative addition of PA to compounds **5** or **8** can not be ruled out,[47] it has not considered because we have failed to observe any rhodium-hydride species and to detect the compound 1,4-diphenylbuta-1,3-diyne in the reaction mixture (GC/MS evidence). The formation of a rhodium-vinyl propagating species from the alkynyl complex **8** having a protonated hemilabile ligand can follow several paths and some of them are shown in Scheme 4: i) direct insertion of the η^2-coordinated monomer into the rhodium-alkynyl bond, ii) migration of the alkynyl ligand to the electrophillic α carbon of the vinylidene ligand resulting from the tautomerization of a η^2-alkyne ligand, and iii) proton transfer from the NH group to the η^2-coordinated monomer.[48]

The three potential pathways have some precedent in the literature. The insertion of internal alkynes into a alkynyl-rhodium(I) complex have been proposed in the mechanism of rhodium-

catalyzed hydroalkynylation of internal alkynes with silylacetylenes.[49] On the other hand, the formation of rhodium and ruthenium enynyl complexes by coupling of alkynyl and vinylidene C_2 fragments is well documented in stoichiometric reactions.[50,51] Finally, vinyl- alkynyl- rhodium(III) species are also common in rhodium alkyne chemistry.[50,52] However, pathway iii is unlikely to occur as it involves the participation of a vinyl-Rh(III) complex as propagating species. This is further supported for the coupling constant exhibited by the minor species at δ 18.01 ppm (J_{P-Rh} = 143.7 Hz) in Figure 11, that could be tentatively assigned to the active propagating species, which suggests a rhodium(I) species.

Interestingly the NH function of the protonated hemilabile ligand could also play an important role in the termination step (pathways i and ii) through the direct protonation of the vinyl propagating species or, alternatively, by protonation of the rhodium center followed by reductive elimination. In fact, we routinely isolate the PPA polymers free of any rhodium species (^{31}P NMR evidence) without the need of diluted acetic acid solutions to quench the polymerization.
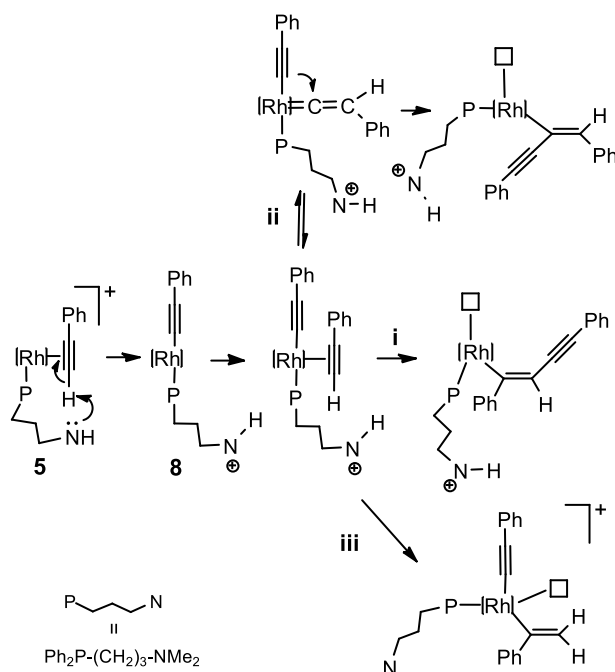
Scheme 4

Conclusions

The present study has shown that rhodium complexes [Rh(diene){Ph$_2$P(CH$_2$)$_n$Z}]$^+$ containing functionalized phosphine ligands of hemilabile character of the type Ph$_2$P(CH$_2$)$_n$Z (Z = OMe, NMe$_2$, SMe; n = 2, 3) exhibit a great activity for PA polymerization. The obtained PPAs show a *cis-transoidal* configuration with a high level of steroregularity. The more efficient catalytic systems are the complexes [Rh(diene){Ph$_2$P(CH$_2$)$_3$NMe$_2$}]$^+$ (diene = nbd and tfb) that afford very high molecular weight PPA with moderate polydispersity indexes. However, in the presence of DMAP both catalysts gave low molecular weight PPA with a narrowest molecular weight distribution. Multistage polymerization and co-polymerization experiments have demonstrated the quasi-living nature of PA polymerization under these conditions.

The investigation of PA polymerization by spectroscopic means, under stoichiometric and catalytic conditions, has revealed the active role of the hemilabile phosphine ligand both in the initiation and, probably, in the termination steps through proton transfer processes involving the hemilabile fragment of the ligand. The intramolecular proton transfer from a η^2-alkyne ligand to the hemilabile ligand gives a cationic alkynyl intermediate which is most likely involved in the generation of very stable rhodium-vinyl species responsible for the propagation step. On the other hand, the direct protonation of the vinyl propagating species by the protonated hemilabile ligand could also be operative in the termination step. Further work in the development of new polymerization catalyst precursors based on the design of hemilabile ligands is currently in progress.

Experimental Section

Scientific Equipment. C, H and N analyses were carried out in a Perkin-Elmer 2400 CHNS/O analyzer. NMR spectra were recorded on Bruker Avance 300 or 400 MHz spectrometers; unless otherwise stated all NMR measurements were carried at 298 K in CDCl$_3$. ^{1}H (300.13, 400.13 MHz), ^{19}F (282.4 MHz), ^{31}P{^{1}H} (121.48, 161.97 MHz) and ^{13}C{^{1}H} (75.48, 100.61 MHz) NMR chemical shifts are reported in ppm relative to tetramethylsilane and referenced to partially deuterated solvent resonances for ^{1}H and ^{13}C, CCl$_3$F for ^{19}F, and H$_3$PO$_4$ (85%) for ^{31}P. Coupling

constants (J) are given in Hertz. FAB mass spectra were recorded on a VG Autospec double-focusing mass spectrometer. The ions were produced by the standard Cs^+ gun at *ca*. 30 KV; 3-nitrobenzyl alcohol (NBA) was used as matrix. Electrospray mass spectra (ESI-MS) were recorded in methanol on a Bruker MicroTof-Q using sodium formiate as reference. MALDI-Tof mass spectra were obtained on a Bruker Miocroflex mass spectrometer using DCTB (*trans*-2-[3-(4-*tert*-butylphenyl)-2-methyl-2-propenylidene]malononitrile) or dithranol as matrix.

FT-IR spectra were collected on a Nicolet Nexus 5700 FT spectrophotometer equipped with a Nicolet Smart Collector diffuse reflectance accessory. Thermal gravimetric analyses were carried out on a TA Q-5000 TGA apparatus (TA Instruments). Samples were heated under nitrogen from room temperature to 600ºC at a rate of 10ºC/min and then heated under air up to 750ºC at the same rate. Differential scanning calorimetry experiments were carried out on a DSC Q-20 apparatus (TA Instruments). Samples were heated under nitrogen from -40ºC to 200ºC at a rate of 10ºC/min and cooled to the initial temperature at the same rate. In some experiments this cycle was repeated several times. PPA samples for IR and thermal analysis were prepared dissolving PPA (5 mg) in THF (0.2 mL) and the solution mixed with KBr (50 mg). Then, the solvent was evaporated under vacuum to produce a yellow solid that was ground into a fine powder. The molecular weights (M_n and M_w) and polydispersity indices (M_w/M_n) of PPA samples were measured by GPC with a Waters 2695 autosampler chromatograph equipped with Phenogel linear mixed columns × 2, and a Waters 2487 dual lambda UV detector, which was previously calibrated with polystyrene standards (molecular weight limit up to 1×10^7). The samples were eluted at 35ºC with THF at a flow rate of 1 mL/min.

Synthesis. All experiments were carried out under an atmosphere of argon using Schlenk techniques. Solvents were obtained from a Solvent Purification System (Innovative Technologies). HC≡CPh was purchased from Aldrich and flash distilled over CaH_2 prior to use. Standard literature procedures were used to prepare the starting materials [Rh(μ-Cl)(diene)]$_2$ (diene = cod,[53] nbd,[54] tfb[55]). The functionalized phosphines $Ph_2P(CH_2)_nZ$ (Z = OMe, SMe, NMe_2) were prepared following published methods.[23,56]

Polymerization Reactions. The polymerization reactions were carried out under an argon atmosphere in Schlenk tubes (10 mL). A typical polymerization procedure is as follows: phenylacetylene (70 μL, 0.64 mmol) was added to a THF solution (2.5 mL) of [Rh(diene){Ph$_2$P(CH$_2$)$_n$Z}]BF$_4$ (6.4 μmol) and the mixture stirred at 30 °C. The progress of the reaction was monitored by the consumption of monomer controlled by GC using octane as internal standard. The polymer was isolated by precipitation with methanol (10 mL), washed with methanol, and dried under vacuum to constant weight.

General Procedure for the Preparation of the Complexes [Rh(diene){Ph$_2$P(CH$_2$)$_n$Z}]BF$_4$ (1–7). *Method A*. A suspension of [Rh(μ-Cl)(diene)]$_2$ (0.500 mmol) in acetone (10 mL) or THF was treated with AgBF$_4$ (194 mg, 1.00 mmol) to give orange suspensions. The AgCl was removed by filtration and the resulting orange solution, containing the solvato species [Rh(diene)(Me$_2$CO)$_n$]$^+$, poured into an acetone solution of Ph$_2$P(CH$_2$)$_n$Z (1.00 mmol) and stirred for 2 hours at room temperature. The solvent was removed under vacuum and the residue stirred and washed with diethyl ether (3 x 5 mL). The compounds were isolated by filtration and obtained as yellow/orange solids. *Method B*. Solid [Rh(μ-Cl)(diene)]$_2$ (0.500 mmol) was added to a solution of the corresponding Ph$_2$P(CH$_2$)$_n$Z (1.00 mmol) in acetone or THF (10 mL) to give yellow/orange solutions of the complexes [RhCl(diene){Ph$_2$P(CH$_2$)$_n$Z}]. Further reaction with AgBF$_4$ (194 mg, 1.00 mmol) afforded orange suspensions from which the compounds were isolated following the procedure described above. Crude products were recrystallized by layering diethyl ether on a saturated solution of the compounds in acetone or tetrahydrofuran. Although most compounds can be obtained by both methods in similar yields, the reported yield corresponds, unless otherwise stated, to the obtained using Method A in acetone.

[Rh(cod){Ph$_2$P(CH$_2$)$_2$OMe}]BF$_4$ (1). Yield: 65 % (Method A), 63 % (Method B). Anal. Calcd for C$_{23}$H$_{29}$BF$_4$OPRh: C, 50.95; H, 5.39. Found: C, 50.71; H, 4.87. MS (FAB+, *m/z*, %): 455 ([M]$^.$, 70). ^{1}H NMR: δ 7.66–7.27 (m, 10H, Ph), 5.44 (br, 2H, =CH cod), 3.79 (dt, J_{H-P} = 21.2, J_{H-H} = 5.9, 2H, CH$_2$P), 3.67 (s, 3H, OMe), 3.41 (br, 2H, =CH cod), 2.87 (dt, J_{H-P} = 9.5, J_{H-H} = 5.9, 2H, CH$_2$O),

2.52 (m br, 4H, CH_2 cod), 2.06 (m br, 4H, CH_2 cod). $^{31}P\{^1H\}$ NMR: δ 40.89 (d, J_{P-Rh} = 151.5). $^{13}C\{^1H\}$ NMR: δ 132.91 (d, J_{C-P} = 11.4, C_o), 132.02 (C_p), 129.64 (d, J_{C-P} = 10.4, C_m), 127.47 (d, J_{C-P} = 46.0, C_i), 108.28 (dd, J_{C-Rh} = 9.6, J_{C-P} = 7.0, =CH cod), 75.13 (CH_2), 68.95 (d, J_{C-Rh} = 15.5, =CH cod), 64.49 (OMe), 32.41 (CH_2 cod), 28.45 (d, J_{C-P} = 24.4, CH_2P), 27.77 (CH_2 cod).

[Rh(cod){Ph₂P(CH₂)₂SMe}]BF₄ (2). Yield: 74 %. Anal. Calcd for $C_{23}H_{29}BF_4PRhS$: C, 49.48; H, 5.23. Found: C, 49.62; H, 4.98. MS (MALDI-Tof, DCTB, CH_2Cl_2) m/z = 471 [M][.] ^1H NMR: δ 7.71–7.56 (m, 10H, Ph), 5.34 (br, 4H, =CH cod), 2.66 (s, 3H, SMe), 2.57 (br, 12H, CH_2 cod and CH_2). $^{31}P\{^1H\}$ NMR: δ 64.18 (d, J_{P-Rh} = 161.4)**.** $^{13}C\{^1H\}$ NMR: δ 133.47-128.53 (m, Ph), 107.60 (br, =CH cod), 78.75 (br, =CH cod), 32.36, 29.85 (br, CH_2), 29.65, 27.96 (CH_2 cod), 22.42 (SMe).

[Rh(cod){Ph₂P(CH₂)₂NMe₂}]BF₄ (3). Yield: 87 % (Method A), 88 % (Method B). Anal. Calcd for $C_{24}H_{32}BF_4NPRh$: C, 51.92; H, 5.81; N, 2.52. Found: C, 51.65; H, 5.63; N, 2.32. MS (FAB+, *m/z, %*): 468 ([M][,] 100). ^1H NMR: δ 7.73–7.56 (m, 10H, Ph), 5.32 (br, 2H, =CH cod), 3.60 (br, 2H, =CH cod), 2.77 (s, 6H, NMe₂), 2.72–2.05 (m, 12H, CH_2 cod and CH_2). $^{31}P\{^1H\}$ NMR: δ 42.65 (d, J_{P-Rh} = 169.7). $^{13}C\{^1H\}$ NMR: δ 132.98 (d, J_{C-P} = 11.3, C_o), 131.80 (d, J_{C-P} = 2.4, C_p), 129.63 (d, J_{C-P} = 10.3, C_m), 128.97 (d, J_{C-P} = 39.9, C_i), 107.87 (dd, J_{C-Rh} = 9.7, J_{C-P} = 6.9, =CH cod), 75.53 (d, J_{C-Rh} = 12.2, =CH cod), 62.18 (CH_2N), 49.74 (NMe₂), 31.51, 28.58 (CH_2 cod), 27.55 (d, J_{C-P} = 25.2, CH_2P).

[Rh(cod){Ph₂P(CH₂)₃OMe}]BF₄ (4). Yield: 52 %. Anal. Calcd for $C_{24}H_{31}BF_4OPRh$: C, 51.82; H, 5.61. Found: C, 51.30; H, 5.31. MS (FAB+, *m/z, %*): 469 ([M][,] 100). ^1H NMR: δ 7.68–7.52 (m, 10H, Ph), 5.31 (br, 2H, =CH cod), 4.04 (t, J_{H-H} = 4.8, 2H, CH_2O), 3.31 (s, 3H, OMe), 3.23 (br, 2H, =CH cod), 2.72–2.49 (m, 6H, CH_2 cod and CH_2), 2.12–1.97 (m, 6H, CH_2 cod and CH_2). $^{31}P\{^1H\}$ NMR: δ 20.9 (d, J_{P-Rh} = 149.2). $^{13}C\{^1H\}$ NMR: δ 133.03 (d, J_{C-P} = 10.8, C_o), 131.46 (d, J_{C-P} = 2.1, C_p), 129.27 (d, J_{C-P} = 9.9, C_m), 129,13 (d, J_{C-P} = 44.0, C_i), 107.72 (dd, J_{C-Rh} = 10.1, J_{C-P} = 6.9, =CH cod), 76.51 (CH_2O), 70.71 (d, J_{C-Rh} = 15.2, =CH cod), 62.38 (OMe), 32.55 (d, J_{C-P} = 2.3, CH_2 cod), 27.73 (CH_2 cod), 24.16 (d, J_{C-P} = 25.1, CH_2P), 22.91 (CH_2).

[Rh(cod){Ph₂P(CH₂)₃NMe₂}]BF₄ (5). Method A was carried out at 273 K . Yield: 63 %. Anal. Calcd for $C_{25}H_{34}BF_4NPRh$: C, 52.75; H, 6.02; N, 2.46. Found: C, 52.77; H, 5.91; N, 2.12. MS

(FAB+, *m/z*, %): 482 ([M]·, 100). ^{1}H NMR: δ 7.58–7.42 (m, 10H, Ph), 5.31 (br, 2H, =CH cod), 3.14 (br, 2H, =CH cod), 2.86 (br, 2H, CH$_2$N), 2.40 (m, 6H, CH$_2$ cod and CH$_2$), 2.34 (s, 6H, NMe$_2$), 1.94 (m, 6H, CH$_2$ cod and CH$_2$). ^{31}P{^{1}H} NMR: δ 17.92 (d, $J_{\text{P-Rh}}$ = 155.7). ^{13}C{^{1}H} NMR: δ 133.49 (d, $J_{\text{C-P}}$ = 10.2, C$_o$), 131.50 (d, $J_{\text{C-P}}$ = 2.1, C$_p$), 129.59 (d, $J_{\text{C-P}}$ = 44.3, C$_i$), 129.28 (d, $J_{\text{C-P}}$ = 9.8, C$_m$), 106.97 (dd, $J_{\text{C-Rh}}$ = 9.6, $J_{\text{C-P}}$ = 7.1, =CH cod), 74.22 (d, $J_{\text{C-Rh}}$ = 12.8, =CH cod), 64.95 (d, $J_{\text{C-P}}$ = 5.7, CH$_2$), 51.25 (NMe$_2$), 31.66, 28.72 (CH$_2$ cod), 27.87 (d, $J_{\text{C-P}}$ = 24.6, CH$_2$P), 20.50 (CH$_2$).

[Rh(tfb){Ph$_2$P(CH$_2$)$_3$NMe$_2$}]BF$_4$ (6). Yield: 55 %. Anal. Calcd for C$_{29}$H$_{28}$BF$_8$NPRh: C, 50.70; H, 4.07; N, 2.04. Found: C, 50.97; H, 4.52; N, 2.02. MS (ESI+, CH$_2$Cl$_2$, *m/z*): 600 ([M]·). ^{1}H NMR: δ 7.65–7.46 (m, 10H, Ph), 5.87 (br, 2H, CH tfb), 5.44 (br, 2H, =CH tfb), 3.00 (br, 4H, =CH tfb and CH$_2$N), 2.55 (m, 2H, CH$_2$P), 2.46 (s, 6H, NMe$_2$), 1.84 (m, 2H, CH$_2$). ^{31}P{^{1}H} NMR: δ 23.07 (d, $J_{\text{P-Rh}}$ = 173.7). ^{19}F NMR (298 K, CDCl$_3$): δ -148.46 (m, 2F tfb), -152.49 (s, 4F BF$_4$), -161.23 (m, 2F tfb). ^{13}C{^{1}H} NMR: δ 142.76, 139.61 (d, $J_{\text{C-F}}$ = 133.5, 140.4, tfb), 133.09 (d, $J_{\text{C-P}}$ = 11.1, C$_o$), 131.56 (d, $J_{\text{C-P}}$ = 2.1, C$_p$), 129.48 (d, $J_{\text{C-P}}$ = 10.2, C$_m$), 128.84 (d, $J_{\text{C-P}}$ = 47.5, C$_i$), 92.58 (dd, $J_{\text{C-Rh}}$ = 10.4, J_{CP} = 5.5, =CH tfb), 64.16 (d, $J_{\text{C-P}}$ = 5.0, CH$_2$), 57.74 (d, $J_{\text{C-Rh}}$ = 11.2, =CH tfb), 51.34 (NMe$_2$), 41.48 (CH tfb), 22.10 (d, $J_{\text{C-P}}$ = 25.1, CH$_2$P), 20.83 (CH$_2$).

[Rh(nbd){Ph$_2$P(CH$_2$)$_3$NMe$_2$}]BF$_4$ (7). Yield: 61 %. Anal. Calcd for C$_{24}$H$_{30}$BF$_4$NPRh: C, 52.11; H; 5.47; N, 2.53. Found: C, 52.24; H, 5.53; N, 2.51. MS (ESI+, CH$_2$Cl$_2$,) *m/z*: 466. (M·). ^{1}H NMR (298 K, CD$_2$Cl$_2$): δ 7.65–7.53 (m, 10H, Ph), 5.38 (br, 2H, =CH nbd), 3.96 (br, 2H, CH nbd) 3.35 (br, 2H =CH nbd), 2.80 (m, 2H, CH$_2$N), 2.43 (m, 2H, CH$_2$P), 2.37 (6H, NMe$_2$), 1.82 (m, 2H, CH$_2$), 1.55 (br, 2H, CH$_2$ nbd). ^{31}P{^{1}H} NMR (298 K, CD$_2$Cl$_2$): δ 21.52 (d, $J_{\text{P-Rh}}$ = 172.5). ^{13}C{^{1}H} NMR (298 K, CD$_2$Cl$_2$): δ 133.01 (d, $J_{\text{C-P}}$ = 11.1, C$_o$), 131.45 (d, $J_{\text{C-P}}$ = 2.3, C$_p$), 129.36 (d, $J_{\text{C-P}}$ = 10.1, C$_m$), 129.01 (d, $J_{\text{C-P}}$ = 41.0, C$_i$), 92.43 (dd, $J_{\text{C-Rh}}$ = 9.5, $J_{\text{C-P}}$ = 5.2, =CH nbd), 66.27 (d $J_{\text{C-P}}$ = 6.2 CH$_2$ nbd), 64.82 (d, $J_{\text{C-P}}$ = 4.8, CH$_2$N), 59.60 (d, $J_{\text{C-Rh}}$ = 10.8, =CH nbd), 52.19 (CH nbd), 50.51 (NMe$_2$), 22.70 (d, $J_{\text{C-P}}$ = 25.0, CH$_2$P), 20.61 (d, $J_{\text{C-P}}$ = 2.8, CH$_2$).

Reaction of [Rh(cod){Ph$_2$P(CH$_2$)$_2$NMe$_2$}]BF$_4$ (5) with PA. To a solution of **5** (10.0 mg, 0.018 mmol) in CD$_2$Cl$_2$ (0.5 mL, NMR tube) at 195 K, was added PA (0.37 mmol). The NMR

measurements at 243 K, recorded immediately after the addition, showed the formation of

[Rh(C≡C-Ph)(cod){Ph$_2$P(CH$_2$)$_3$NHMe$_2$}]BF$_4$ (**8**). ^{1}H NMR (243K, CD$_2$Cl$_2$): δ 8.54 (br, 1H,

N*H*Me$_2$), 7.51–7.35 (m, 15H, Ph), 5.56 (br, 2H, =CH cod), 3.80 (br, 2H, =CH cod), 3.62 (m, 2H,

CH$_2$), 2.76 (s, 6H, NMe$_2$), 2.55 (m, 2H, CH$_2$ cod), 2.41–2.33 (m, 8H, CH$_2$ cod and CH$_2$), 2.14 (m,

2H, CH$_2$). ^{31}P{^{1}H} NMR (243K, CD$_2$Cl$_2$): δ 23.51 (d, J_{P-Rh} = 158.34). ^{13}C{^{1}H} NMR (243K,

CD$_2$Cl$_2$): δ 135.24, 135.10 (CH), 134.71 (C$_i$), 134.04, 132.71, 131.02, 130.58 (CH), 128.16 (C$_i$),

122.18 (dd, J_{C-Rh} = 48.7, J_{CP} = 21.8, *C*≡C), 120.30 (d, J_{C-Rh} = 17.9, C≡*C*), 101.01 (dd, J_{C-Rh} = 10.9, J_{C-P}

= 7.3, =CH cod), 89.08 (d, J_{C-Rh} = 8.1, =CH cod), 59.15 (d, J_{C-P} = 10.3, CH$_2$), 44.95 (NMe$_2$), 33.65,

33.15 (CH$_2$ cod), 27.78 (d, J_{C-P} = 25.8, CH$_2$P), 24.43 (d, J_{C-P} = 2.5, CH$_2$).

Reaction of [Rh(diene){Ph$_2$P(CH$_2$)$_3$NMe$_2$}]BF$_4$ with DMAP. An NMR tube was charged with

[Rh(diene){Ph$_2$P(CH$_2$)$_3$NMe$_2$}]BF$_4$ (diene = tfb, **6**; cod, **5**) (0.02 mmol) and DMAP (2.4 mg, 0.02

mmol) in CD$_2$Cl$_2$ (0.5 mL) at RT. NMR data revealed the formation of compounds

[Rh(diene)(DMAP){Ph$_2$P(CH$_2$)$_3$NMe$_2$}]BF$_4$ (diene = tfb, **9**; cod, **10**). MS and NMR data for **9**: MS

(MALDI-Tof, Dithranol, CD$_2$Cl$_2$, *m/z*): 600.1 ([M – DMAP]$^-$). ^{1}H NMR (298 K, CD$_2$Cl$_2$): δ 8.07 (d,

J_{H-H} = 6.0, 2H, DMAP), 7.65–7.56 (m, 10H, Ph), 6.53 (d, J_{H-H} = 6.0, 2H, DMAP), 5.84 (br, 2H, CH

tfb), 5.24 (br, 4H, =CH tfb), 3.02 (s, 6H, DMAP), 2.88 (m, 2H, CH$_2$), 2.40 (s, 8H, NMe$_2$, CH$_2$),

1.80 (m, 2H, CH$_2$). ^{31}P{^{1}H} NMR (213K, CD$_2$Cl$_2$): δ 24.37 (d, J_{P-Rh} = 176.7). ^{19}F NMR (298 K,

CD$_2$Cl$_2$): δ -147.05 (m, 2F tfb), -152.49 (s, 4F BF$_4$), -159.86 (m, 2F tfb). ^{13}C{^{1}H} NMR (213 K,

CD$_2$Cl$_2$): δ 154.58 (C DMAP), 148.96 (CH DMAP), 141.09, 137.79 (d, J_{C-F} = 133.5, 140.4, C tfb),

132.93 (d, J_{C-P} = 11.0, C$_o$), 131.44 (C$_p$), 129.38 (d, J_{C-P} = 10.1, C$_m$), 127.86 (CH DMAP), 126.32

(C$_i$), 107.23 (m br, =CH tfb), 63.75 (CH$_2$), 50.23 (NMe$_2$), 41.38 (m br, CH tfb), 39.03 (NMe$_2$

DMAP), 22.48 (d, J_{C-P} = 26.0, CH$_2$P), 21.05 (CH$_2$). MS and NMR data for **10**: MS (ESI+,

CH$_2$Cl$_2$/MeOH, *m/z*): 482.3 ([M – DMAP]$^-$). ^{1}H NMR (253 K, CD$_2$Cl$_2$): δ 7.65 (br, 2H, DMAP),

7.56–7.42 (m, 10H, Ph), 6.28 (br, 2H, DMAP), 4.74 (br, 2H, =CH cod), 3.88 (br, 2H, =CH cod),

2.92 (s, 6H, DMAP), 2.47 (m, 4H, CH$_2$ cod), 2.13–1.92 (m, 14H, NMe$_2$, CH$_2$, CH$_2$ cod), 1.28 (br,

2H, CH$_2$). ^{31}P{^{1}H} NMR (253K, CD$_2$Cl$_2$): δ 19.87 (J_{P-Rh} = 151.4). ^{13}C{^{1}H} NMR (253 K, CD$_2$Cl$_2$): δ

153.82 (C DMAP), 148.94 (CH DMAP), 133.17 (d, J_{C-P} = 11.0, C_o), 130.92 (C_p), 129.13 (d, J_{C-P} = 9.6, C_m), 129.65 (d, J_{C-P} = 40.90, C_i), 108.01 (CH DMAP), 103.52 (m, =CH cod), 78.35 (d, J_{C-Rh} = 11.5, =CH cod), 60.16 (d, J_{C-P} = 13.1, CH_2N), 45.32 (NMe_2), 39.33 (NMe_2 DMAP), 32.14, 29.16 (CH_2 cod), 22.81 (d, J_{C-P} = 23.4, CH_2P), 22.5 (d, J_{C-P} = 2.7, CH_2).

Reaction of 5 with DMAP and PA. To a suspension of **5** (11 mg, 0.02 mmol) and DMAP (2.4 mg, 0.02 mmol) in 0.5 mL of THF-d_8 (NMR tube) at 195 K was added PA (0.4 mmol). The solution was stirred at RT for 5 min and then cooled at 243 K. NMR data revealed the formation of compound [Rh(C≡C-Ph)(cod){$Ph_2P(CH_2)_3NMe_2$}] (**11**) and [HDMAP]$^+$. NMR data for **11**: ^{1}H NMR (243 K, THF-d_8): δ 7.61–6.51 (m, 15H, Ph), 5.46 (br, 2H, =CH cod), 3.47 (br, 2H, =CH cod), 2.48–1.60 (set of m, 20H, NMe_2, CH_2 cod and CH_2). ^{31}P{^{1}H} NMR (243 K, THF-d_8): δ 25.56 (d, J_{P-Rh} = 158.9). ^{13}C{^{1}H} NMR (243 K, THF-d_8): 133.00 (d, J_{C-P} = 37.7, C_i), 133.10 (d, J_{C-P} = 11.1, C_o), 128.57 (C_p), 127.68, 127.19 (CH), 126.10 (d, J_{C-P} = 8.7, C_m), 125.66 (CH), 119.47 (dd, J_{C-Rh} = 46.0, J_{C-P} = 22.9, C≡C), 115.51 (d, J_{C-Rh} = 13.3, C≡C), 94.80 (m, =CH cod), 81.94 (d, J_{C-Rh} = 8.0, =CH cod), 58.12 (CH_2), 42.64 (NMe_2), 29.40, 28.53 (CH_2 cod), 25.44 (d, J_{C-P} = 27.5, CH_2P), 23.70 (CH_2). NMR data for [HDMAP]$^+$: ^{1}H NMR (243 K, THF-d_8): δ 10.34 (br, 1H, NH), 8.04 (d, J_{H-H} = 5.7, 2H, CH), 6.52 (d, J_{H-H} = 5.7, 2H, CH), 2.87 (s, 6H, NMe_2). ^{13}C{^{1}H} NMR (243 K, THF-d_8): 152.85, 145.43 (CH), 105.15 (CH), 36.56 (NMe_2).

X-ray Structural Determination of Compounds [Rh(cod){$Ph_2P(CH_2)_3NMe_2$}]BF$_4$ (5) and [Rh(tfb){$Ph_2P(CH_2)_3NMe_2$}]BF$_4$ (6). Suitable crystals for X-ray diffraction were obtained by diffusion of diethylether into THF (**5**) or chloroform (**6**) solutions of the complexes. Data collection (Bruker SMART CCD) and refinement (SHELXL97[57]) were carried out with analogous strategies to those previously reported.[58] In **5** the BF$_4$ anion and a THF molecule exhibited static disorder; full details on the established disorder model are described in the supplementary material. **Crystal data for 5:** $C_{25}H_{34}BF_4NPRh$ · ½ C_4H_8O; triclinic, *P* -1; *a* = 9.4341(6), *b* = 9.8954(6), *c* = 14.835(1) Å, $α$ = 92.365(1), $β$ = 107.922(1), $γ$ = 95.181(1)º, Z = 2; D_c = 1.536 g/cm^3; $μ$ = 0.761 mm^{-1}, min. & max. trans. fact. 0.876 and 0.909; $2θ_{max}$ = 56.66º; 15771 reflec. collected, 6202

unique [R_{int} = 0.0279]; data/restrains/parameters 6202/26/372; final *GoF* 1.007, *R*1 = 0.0392 [5631

reflections, $I > 2\sigma(I)$], w*R*2 = 0.0939 for all data. **Crystal data for 6:** $C_{29}H_{28}BF_8NPRh \cdot CHCl_3$;

monoclinic, $P2_1/n$; *a* = 12.355(2), *b* = 19.720(3), *c* = 12.934(2) Å, β = 93.830(3)°; *Z* = 4;

D_c = 1.704 g/cm^3; μ = 0.92 mm^{-1}, min. & max. trans. fact. 0.859 and 0.959; $2\theta_{max}$ = 57.40°; 20465

reflec. collected, 7435 unique [R_{int} = 0.0654]; data/restrains/parameters 7435/0/410; final *GoF*

1.027, *R*1 = 0.0537 [4813 reflections, $I > 2\sigma(I)$], w*R*2 = 0.112 for all data.

Supporting Information Available: X-ray crystallographic information files containing full

details of the structural analysis of complexes **5** and **6** (CIF format), and Table 2 (solvent effect on

the polymerization of PA catalyzed by **5**). This material is available free of charge via Internet at

http://pubs.acs.org.

References

(1) (a) MacDiarmid, A. G. Curr. Appl. Phys. 2001, 1, 269–279. (b) Naarmann, H. In Polymers,

Electrically Conducting In Ullmann's Encyclopedia of Industrial Chemistry, 6th ed.; Wiley-VCH:

Weinheim, 2002, A21, 429–447.

(2) Gruber, A. S.; Boiteux, G.; de Souza, R. F.; de Souza, M. O. *Polym. Bull.* **2002**, *47*, 529–537.

(3) (a) Aoki, T.; Kaneko, T.; Teraguchi, M. *Polymer* **2006**, *47*, 4867–4892. (b) Tang, B. Z.; Lam,

J. W. Y. *Acc. Chem. Res.* **2005**, *38*, 745–754. (c) Choi, S.-K.; Gal, Y. -S.; Jin, S. -H.; Kim, H. K.

Chem. Rev. **2000**, *100*, 1645–1682.

(4) Trepka, W. J.; Sonnenfeld, R. J. *J. Polym. Sci., Part A-1:Polym. Chem.* **1970**, *8*, 2721–2244.

(5) Shirakawa, H.; Masuda, T.; Takeda, K. In: *The Chemistry of Triple-Bonded Functional Groups*, Supplement C2, Patai, S. Ed.; Wiley: Chichester, **1994**, Chap. 17.

(6) (a) Schrock R. R. *Chem. Commun.* **2005**, 2773–2777. (b) Schrock, R. R.; Luo, S.; Lee, J. C.; Zanetti, N.; Davis, W. M. *J. Am. Chem. Soc.* **1996**, *118*, 3883–3895. (c) Buchmeiser, M.; Schrock, R. R. *Macromolecules* **1995**, *28*, 6642–6649.

(7) (a) Hayano S.; Masuda, T. *Macromolecules* **1998**, *31*, 3170–3174. (b) Nakano, M.; Masuda, T.; Higashimura, T. *Macromolecules* **1994**, *27*, 1344–1348.

(8) Nakayama, Y.; Mashima, K.; Nakamura, A. *Macromolecules* **1993**, *26*, 6267–6272.

(9) (a) Chen, S.; Li, Y.; Zhao, J.; Li, X. *Inorg. Chem.* **2009**, *48*, 1198–1206. (b) Nishiura, M.; Hou, Z. *J. Mol. Catal. A: Chem.* **2004**, *213*, 101–106. (c) Komatsu, H.; Suzuki, Y.; Yamazaki, H. *Chem. Lett.* **2001**, 998–999. (d) Lamata, M. P.; San Jose, E.; Carmona, D.; Lahoz, F. J.; Atencio, R.; Oro, L. A. *Organometallics* **1996**, *15*, 4852–4856. (e) Werner, H.; Schäfer, M.; Wolf, J.; Peters, K.; von Schnering, H. G. *Angew. Chem., Int. Ed. Engl.* **1995**, *34*, 191-194. (f) Schäfer, H. -A.; Marcy, R.; Rüping, T.; Singer, H. *J. Organometallic Chem.* **1982**, *240*, 17–25.

(10) Taube, R.; Sylvester, G. In *Applied Homogeneous Catalysis with Organometallic Compounds*, 2nd ed.; Cornils, B., Herrmann, W. A. Eds.; Wiley-VCH: Weinheim, **2002**, *1*, p. 285.

(11) a) Furlani, A.; Napoletano, C.; Russo, M. V.; Camus, A.; Marsich, N. *J. Polym. Sci., Part A: Polym. Chem.* **1989**, *27*, 75–86. b) Furlani, A.; Napoletano, C.; Russo, M. V.; Feast, W. *J. Polym. Bull.* **1986**, *16*, 311–317.

(12) Katayama, H.; Yamamura, K.; Miyaki, Y.; Ozawa, F. *Organometallics* **1997**, *16*, 4497–4500.

(13) (a) Goldberg, Y.; Alper, H. *J. Chem. Soc., Chem. Commun.* **1994**, 1209–1210. (b) Kishimoto, Y.; Itou, M.; Miyatake, T.; Ikariya, T.; Noyori, R. *Macromolecules* **1995**, *28*, 6662–6666.

(14) (a) H. -J. Haupt and U. Ortmarm, Z. *Anorg. Allg. Chem.,* **1993**, *619,* 1209–1213. (b) Schniedermeier, J., Haupt, H. -J. *J. Organomet. Chem.* **1996**, *506*, 41–47.

(15) Zhang, Y.; Wang, D.; Wurst, K.; Buchmeiser M. R. *J. Organomet. Chem.* **2005**, *609*, 5728–5735.

(16) (a) Kishimoto, Y.; Eckerle, P.; Miyatake, T.; Ikariya, T.; Noyori, R. *J. Am. Chem. Soc.* **1994**, *116*, 12131–12132. (b) Kishimoto, Y.; Miyatake, T.; Ikariya, T.; Noyori, R. *Macromolecules* **1996**, *29*, 5054–5055. (c) Kishimoto, Y.; Eckerle, P.; Miyatake, T.; Kainosho, M.; Ono, A.; Ikariya, T.; Noyori, R. *J. Am. Chem. Soc.* **1999**, *121*, 12035–12044.

(17) (a) Misumi, Y.; Masuda T. *Macromolecules* **1998**, *31*, 7572–7573. (b) Misumi, Y.; Kanki, K.; Miyake, M.; Masuda, T. *Macromol. Chem. Phys.* **2000**, *201*, 2239–2244.

(18) Miyake, M.; Misumi, Y.; Masuda, T. *Macromolecules* **2000**, *33*, 6636–6639.

(19) Saeed, I.; Shiotsuki, M.; Masuda, T. *Macromolecules* **2006**, *39*, 8567–8573.

(20) (a) Jiménez, M. V.; Pérez-Torrente, J. J.; Bartolomé, M. I.; Gierz, V.; Lahoz, F. J.; Oro, L. A. *Organometallics* **2008**, *27*, 224–234. (b) Jiménez, M. V.; Rangel-Salas, I. I.; Lahoz, F. J.; Oro, L. A. *Organometallics* **2008**, *27,* 4229 – 4237.

(21) (a) Braunstein, P.; Naud, F. *Angew. Chem. Int. Ed.* **2001**, *40*, 680-699. (b) Braunstein, P.; Knorr, M.; Stern, C. *Coord. Chem. Rev.* **1998**, *178-180*, 903–965. (c) Bader, A.; Lindner, E. *Coord. Chem. Rev.* **1991**, *108*, 27–110.

(22) Espinet, P.; Soulantica, K. *Coord. Chem. Rev.* **1999**, *193-195*, 499–556.

(23) Jiménez, M. V.; Pérez-Torrente, J. J.; Bartolomé, M. I.; Oro, L. A. *Synthesis* **2009**, 1916–1922.

(24) Initiation efficiency, *IE = M_{theor}/M_n x 100*; where *M_{theor} = [PA]$_0$/[Rh] x $MW_{phenylacetylene}$ x polymer yield*.

(25) Cametti, C.; Codastefano, P.; D'Amato, R.; Furlani, A.; Russo, M. V. *Synth. Met.* **2000**, *114*, 173–179.

(26) Rédrová, D.; Sedláček, J. Žigon, M.; Vohlídal, J. *Collect. Czech. Chem. Commun.* **2005**, *70*, 1787–1798.

(27) Saeed, I.; Shiotsuki, M.; Masuda, T. *Macromolecules* **2006**, *39*, 8977–8981.

(28) Polydispersity indexes, M_w/M_n, in the range 1.05–1.15 are indicative of a living polymerization: Matyjaszewski, K. *Macromolecules* **1993**, *26*, 1787–1788.

(29) *Cis-transoidal* PPA: ^{1}H NMR (CDCl$_3$): δ = 6.90 (m, *m*-H and *p*-H, Ph), 6.61 (*o*-H, Ph), 5.82 (C=CH). ^{13}C NMR (CDCl$_3$): δ = 126.70 (*p*-Ph), 127.58 and 127.80 (*m*- and *p*-Ph), 131.79 (C=CH), 139.36 and 142.90 (quaternary carbons).

(30) The *%* cis content in *cis-transoidal* PPA samples was determined using the following equation: *% cis = 100x($A_{5.82}$x6)/(A_{total})* where $A_{5.82}$ is the area of the vinyl proton and A_{total} is the total area of the spectrum (reference 11).

(31) Fujita, Y.; Misumi, Y.; Tabata, M.; Masuda, T. *J. Polym. Sci, Part A: Pol. Chem.* **1998**, *36*, 3157–3163.

(32) Vosloo, H. C. M; Luyt, A. S. *J. Thermal Anal.* **1995**, *44*, 1261–1275.

(33) Tabata, M.; Takamura, H.; Yokota, K.; Nozaki, Y.; Hoshina, T.; Minakawa, H.; Kodaira, K. *Macromolecules* **1994**, *27*, 6234–6236.

(34) (a) Morino, K.; Asari, T.; Maeda, K.; Yashima, E. *J. Polym. Sci., Part A: Polym. Chem.* **2004**, *42*, 4711–4722. (b) Ishii, F., Matsunami, S.; Shibata, T., Kakuchi, T. *J. Polym. Sci., Part B: Polym. Phys.* **1999**, *37*, 1657–1664.

(35) Simionescu, C. I.; Percec, V.; Dumitrescu, S. *J. Polym. Sci. Polym. Chem. Ed.* **1977**, *15*, 2497–2509.

(36) Dega-Szafran, Z.; Kania, A.; Nowak-Wydra, B.; Szafran, M. *J. Mol. Struct.* **1994**, *322*, 223–232.

(37) Mayershoffer, M. G.; Nuyken, O. *J. Polym. Sci., Part A: Polym. Chem.* **2005**, *43*, 5723–5747.

(38) Koga, N.; Morokuma, K. *Chem. Rev.* **1991**, *91*, 823–842.

(39) Li, K.; Wei, G.; Darkwa, J.; Pollack, S. K. *Macromolecules* **2002**, *35*, 4573–4576.

(40) Tang, B. Z.; Poon, W. H.; Leung, S. M.; Leung, W. H.; Peng, H. *Macromolecules* **1997**, *30*, 2209–2212.

(41) Trzeciak, A. M.; Ziółkowski, J. J. *Appl. Organomet. Chem.* **2004**, *18*, 124–129.

(42) (a) Saeed, I.; Shiotsuki, M.; Masuda, T. *J. Mol. Catal., A: Chem.* **2006**, *254*, 124–130. (b) Katayama, H.; Yamamura, K.; Miyaki, Y.; Ozawa, F. *Organometallics* **1997**, *16*, 4497–5000.

(43) (a) Mastrorilli, P.; Nobile, C. F.; Gallo, V.; Suranna, G. P.; Farinola, G. *J. Mol. Catal., A: Chem.* **2002**, *184*, 73–78. (b) Mitsuyama, M.; Ishii, R.; Kondo, K. *J. Polym. Sci., Part A: Polym. Chem.* **2000**, *38*, 3419–3427.

(44) Grotjahn, D. B. *Chem. Eur. J.* **2005**, *11*, 7146–7153.

(45) PA polymerization reactions by complexes **5**–**7** have also been performed in the presence of BHT (2,6-di-tert-butyl-4-methylphenoxy) giving polymers with the same properties that the obtained without the radical inhibitor. Thus, a radical mechanism has not been considered.

(46) Hirao, K.; Ishii, Y.; Terao, T.; Kishimoto, Y.; Miyatake, T.; Ikariya, T.; Noyori, R. *Macromolecules* **1998**, 31, 3405–3408.

(47) Bianchini, C.; Meli, A.; Peruzzini, M.; Zanobini, F.; Bruneau, C.; Dixneuf, P. H. *Organometallics* **1990**, *9*, 1155–1160.

(48) (a) Dervisi, A.; Edwards, P. G.; Newman, P. D.; Tooze, R. P. *J. Chem. Soc., Dalton Trans*., **2000**, 523–528. (b) Scrivanti, A.; Beghetto, V.; Campagna, E.; Zanato, M.; Matteoli, U. *Organometallics* **1998**, *17*, 630–635.

(49) Nishimura, T.; Guo, X. –X.; Ohnishi, K.; Hayashi, T. *Adv. Synth. Catal.* **2007**, *34*, 2669–2672.

(50) Schäfer, M.; Mahr, N.; Wolf, J.; Werner, H. *Angew. Chem. Int., Ed. Engl.* **1993**, *32*, 1315–1317.

(51) Wakatsuki, Y.; Yamazaki, H.; Kumegawa, H.; Satoh, T.; Satoh, J. Y. *J.. Am. Chem. Soc*. **1991**, *113*, 9604–9610.

(52) Werner, H.; Kukla, F.; Steinert, P. *Eur. J. Inorg. Chem*. **2002**, 1377–1389.

(53) Giordano, G.; Crabtree, R. H. *Inorg. Synth*. **1979**, *19*, 218–219.

(54) Abel, E. W.; Bennett, M. A.; Wilkinson, G. *J. Chem. Soc*. **1959**, 3178–3182.

(55) Roe, D. M.; Massey, A. G. *J. Organomet. Chem*. **1971**, *28*, 273–279.

(56) (a) McEwen, W. E.; Smith, J. H.; Woo E. J. *J. Am. Chem. Soc*. **1980**, *102*, 2746–2751. (b) McEwen, W. E.; Janes, A. B.; Knapczyk, J. W.; Kyllingstad, V. L.; Shiau, W. I.; Shore, S.; Smith

J. H. *J. Am. Chem. Soc.* **1978**, *100*, 7304–7311. (c) Anderson, G. K.; Kumar, R. *Inorg. Chem.* **1984**, *23*, 4064–4068.

(57) SHELXTL *Package* v. 6.10; Bruker AXS; Madison, WI, 2000. Sheldrick, G.M. *SHELXS-86 and SHELXL-97*; University of Göttingen; Göttingen, Germany, 1997.

(58) Alonso, P. J.; Benedí, O.; Fabra, M. J.; Lahoz, F. J.: Oro, L. A.; Pérez-Torrente, J. J. *Inorg. Chem.* **2009**, 48, 7984–7993.

for Table of Contents use only

Cationic Rhodium Complexes with Hemilabile Phosphine Ligands as Polymerization Catalyst for High Molecular Weight Stereoregular Polyphenylacetylene.

M. Victoria Jiménez,* Jesús J. Pérez-Torrente,* M. Isabel Bartolomé, Eugenio Vispe, Fernando J. Lahoz, and Luis A. Oro

Catalyst Diene	cod	tfb	nbd
M_w/M_n	1.62	1.70	1.53
M_n	160 000	970 000	1 420 000
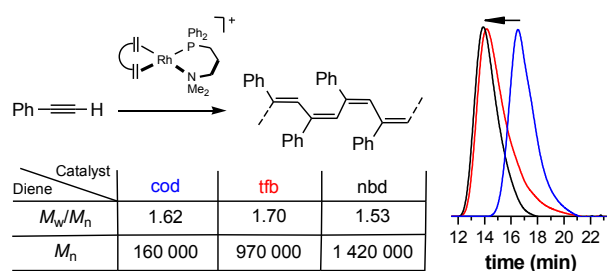
Cationic rhodium(I) complexes containing hemilabile functionalized phosphine ligands of the type $Ph_2P(CH_2)_nZ$ (Z = OMe, NMe_2, SMe; n = 2, 3) showed a great activity for the stereoregular phenylacetylene (PA) polymerization. The complexes $[Rh(diene)\{Ph_2P(CH_2)_3NMe_2\}]^+$ (diene = nbd and tfb) afforded very high molecular weight PPA with moderate polydispersity indexes. In contrast, both catalysts gave low molecular weight PPA in the presence of DMAP (4-(dimethylamino)pyridine) as co-catalyst. Noteworthy, the catalyst with tfb ligand was found to perform PA polymerization almost in a living manner.